Theory of multiexciton dynamics in molecular chains

Luxia Wang*
Department of Physics, University of Science and Technology Beijing, 100083 Beijing, China

Volkhard May†
Institute of Physics, Humboldt-University at Berlin, Newtonstraße 15, D-12489 Berlin, Germany
(Received 15 August 2016; revised manuscript received 11 October 2016; published 10 November 2016)

Ultrafast and strong optical excitation of a molecular system is considered which is formed by a regular one-dimensional arrangement of identical molecules. As it is typical for zinc chlorine-type molecules the transition energy from the ground state to the first excited singlet state is assumed to be smaller than the energy difference between the first excited state and the following one. This enables the creation of many excitons without their immediate quenching due to exciton-exciton annihilation. As a first step into the field of dense Frenkel-exciton systems the present approach stays at a mean-field type of description and ignores vibrational contributions. The resulting nonlinear kinetic equations mix Rabi-type oscillations with those caused by energy transfer and suggest an excitation-dependent narrowing of the exciton band. The indication of this effect in the framework of a two-color pump-probe experiment and of the detection of photon emission is discussed.

DOI: 10.1103/PhysRevB.94.195413

I. INTRODUCTION

Although investigated for decades it is still of interest to uncover details of excitation energy transfer (EET) in dye aggregates, conjugated polymers or supramolecular complexes. The technological importance of EET in photovoltaic cells or light emitting diodes may be the major explanation for the ongoing research (see, for example, the recent overviews [1–3] and Ref. [4]). So-called multiexciton effects which come into play if stronger optical excitation is applied may be another reason for the continuing work. Such studies are of more fundamental character and are related in most cases to exciton-exciton annihilation (recent work is described in Refs. [5–10]). Stronger optical excitation of molecular systems is also of particular interest if the molecules coat a metal nanoparticle. Subsequent plasmon excitation may cause what is described in literature as the SPASER effect [11,12]. Interestingly, theory and simulation of multiexciton phenomena in the molecular system are not of such a degree of elaboration as the description of respective processes in semiconductor nanocrystals and quantum dots (see the somewhat older work of Refs. [13–16] on multiexciton effects). Following our recent attempts in Refs. [17,18] we suggest a theory here which is ready to describe the dynamics of multiple electronic excitations in molecular systems.

We assume that E_{eg} is the energy difference between the ground state (S_0 state) and the first excited singlet state (S_1 state). Moreover, E_{fg} shall label the energy difference between the S_0 state and the higher lying level (S_2 state) of the considered molecules. Exciton-exciton annihilation proceeds if $2E_{eg}$ comes into resonance to a transition into the S_2 state, i.e., $E_{fg} \approx 2E_{eg}$. Considering vibrational excitations, too, this requirement is fulfilled for many types of molecules. Here, however, we will consider molecular species where $2E_{eg}$ is out of resonance to a higher transition. For example, the zinc chlorine molecules studied in [19] fulfill $2E_{eg} < E_{fg}$. As a consequence, excited state absorption from a molecule already excited into its first excited state with the same amount of energy does not take place. And, exciton-exciton annihilation is not possible. Instead the simultaneous excitation of molecules into their first excited state efficiently shall take place. This will be the subject of the subsequent considerations.

Excited state dynamics and excitation-dependent emission spectra will be presented in the following for one-dimensional (1D) molecular systems (nanowires) which have been intensively studied in the literature. Femtosecond pump-probe spectroscopy could be applied to thin films of the quasi-one-dimensional organic semiconductor 3,4,9,10-perylene tetracarboxylic dianhydride (PTCDA) [20]. Long-range exciton migration in individual perylene bisimide J-aggregates has been reported in Ref. [21]. Similar experiments on single perylene-based H-aggregates were described in Ref. [22]. Femtosecond hot exciton emission was detected for the quasi-one-dimensional π-conjugated organic rigid-rod quantum nanowire of methyl-substituted ladder-type poly(para-phenylenes) [8]. Reference [23] describes experiments on EET in cyclic structures of π-conjugated materials covering several monomers. The quoted experimental work motivates the restriction to molecular chains which will consist of up to 25 monomers (cf. also the scheme in Fig. 1).

A consequent quantum theory of a strongly excited molecular system but coupled to a metal nanoparticle has been offered recently in [17,24,25]. This theory handles the dynamics of the strongly excited state of some tens of molecules interacting with the dipole plasmons of a spherical nanoparticle in an exact manner. Moreover, an approximate description which is similar to the one used hereafter and presented in [18] was able to describe the molecule-plasmon system with up to 100 molecules (cf. Ref. [24]). It coincides with the exact approach for lower numbers of molecules (up to 20). This observation encouraged us to use the same approach but without the presence of a metal nanoparticle to study multiexciton effects in a molecular chain. All equations of motion used in the following have been already presented in

*luxiawang@sas.ustb.edu.cn
†may@physik.hu-berlin.de

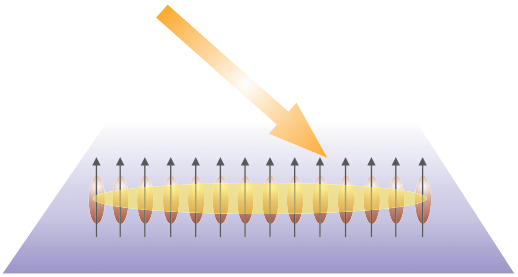

FIG. 1. Scheme of a linear arrangement of identical molecules with transition dipole moment perpendicular to the chain axis (H-aggregate configuration). Optical excitation (orange arrow) may move the molecules into their excited state (yellow sphere).

Ref. [18]. Here, we consider special molecules with $2E_{eg} < E_{fg}$ where exciton-exciton annihilation is of less importance, but study the simultaneous excitation of many molecules into their first excited state beyond a rate-equation-type description and by the inclusion of possible formation of delocalized exciton states. However, the present description ignores the direct consideration of two-exciton correlation. In this sense it represents a type of mean-field theory for the treatment of multiple excitations. Those are accounted for by a nonlinear dependence on the molecular excited state population. We will concentrate on the change of Frenkel-exciton-type states with the strength of ultrafast optical excitation.

The paper is organized as follows. The subsequent Sec. II introduces the model and the used equations of motion to study ultrafast excitation. Photoinduced EET dynamics are considered in Sec. III. A possible spectroscopic detection of the suggested change of the exciton spectrum with excitation strength is discussed in Sec. IV and in the Appendix. Some conclusions are drawn in Sec. V.

II. MODEL AND BASIC KINETIC EQUATIONS

Photoinduced EET kinetics are investigated for a complex of $N_{\rm mol}$ molecules for which the ground state $|\varphi_{mg}\rangle$ with energy E_{mg} and the first excited state $|\varphi_{me}\rangle$ with energy E_{me} are considered (m counts the individual molecules). The overall Hamiltonian including ultrafast laser pulse excitation is written as

$$H(t) = H_{\rm exc} + H_{\rm field}(t). \tag{1}$$

It covers the standard exciton Hamiltonian,

$$H_{\rm exc} = \sum_m E_m B_m^+ B_m + \sum_{m,n} J_{mn} B_m^+ B_n. \tag{2}$$

Here, the ground-state energy has been set equal to zero, and we abbreviated $E_{me} - E_{mg}$ by E_m. The B_m^+ are transition operators $B_m^+ = |\varphi_{me}\rangle\langle\varphi_{mg}|$ moving molecule m from its ground state to its first excited state. Be also aware of the important relation $B_m^+ B_m + B_m B_m^+ = 1$ (completeness relation for the two-level system). The energy transfer (excitonic) coupling has been denoted by J_{mn}. It is used in dipole approximation (justified by the considered values $\Delta r_{\rm mol}$ of intermolecule distances),

$$J_{mn} = \kappa_{mn} d_m d_n / R_{mn}^3. \tag{3}$$

The transition dipole moment of molecule m has been written as $\mathbf{d}_m = d_m \mathbf{e}_m$, and $\mathbf{R}_{mn} = R_{mn}\mathbf{n}_{mn}$ is the distance vector connecting the centers of mass of the two molecules. It results in the following orientation factor $\kappa_{mn} = [\mathbf{e}_m \mathbf{e}_n] - 3[\mathbf{e}_m \mathbf{n}_{mn}][\mathbf{n}_{mn} \mathbf{e}_n]$. The excited states which are covered by the given description are the single excitations of different molecules. A state with N^* excited molecules simply reads

$$|\psi_{N^*}\rangle = B_1^+ \ldots B_{N^*}^+ |\phi_g\rangle. \tag{4}$$

Here, $|\phi_g\rangle$ is the electronic ground state of the whole molecular system (a good approximation would be $|\phi_g\rangle = \prod_m |\varphi_{mg}\rangle$).

The coupling to the laser pulse takes the form,

$$H_{\rm field}(t) = -\mathbf{E}(t) \cdot \sum_m \mathbf{d}_m B_m^+ + \text{H.c.}. \tag{5}$$

The electric-field strength,

$$\mathbf{E}(t) = \mathbf{n}_E E(t) e^{-i\omega_0 t} + \text{c.c.}, \tag{6}$$

refers to a single pulse with unit vector of field polarization $\mathbf{n}_E$, with carrier frequency ω_0, and with pulse envelope,

$$E(t) = E_0 \exp\left(-4 \ln 2 (t - t_{\rm p})^2 / \tau_{\rm p}^2\right). \tag{7}$$

We introduced $\tau_{\rm p}$ as the full width at half maximum (FWHM) of the pulse. To simplify the notation we abbreviate

$$R_m(t) = -\mathbf{E}(t) \cdot \mathbf{d}_m = -\mathbf{n}_E \cdot \mathbf{d}_m E(t) e^{-i\omega_0 t} + \text{c.c.}. \tag{8}$$

Equations of motion

As demonstrated, for example, in Ref. [18] kinetic equations can be derived by considering time-dependent expectation values of different arrangements of the operators B_m^+ and B_n. Therefore, we introduce the arbitrary operator $\hat{O}$. Its expectation value $O(t) = \langle \hat{O} \rangle = \text{tr}\{\hat{\rho}(t)\hat{O}\}$ is defined by the reduced density operator $\hat{\rho}(t)$ which should obey the following quantum master equation:

$$\frac{\partial}{\partial t}\hat{\rho}(t) = -\frac{i}{\hbar}[H(t), \hat{\rho}(t)]_- - \mathcal{D}\hat{\rho}(t). \tag{9}$$

For the sake of simplicity we chose a description where dissipation exclusively appears via a decay of the excited molecular state. The action of the related dissipative superoperator takes the form,

$$\mathcal{D}\hat{\rho}(t) = \sum_m \frac{k_m}{2}([B_m^+ B_m, \hat{\rho}(t)]_+ - 2B_m \hat{\rho}(t) B_m^+), \tag{10}$$

where k_m denotes the decay rate referring to molecule m. In the concrete computations we assume the related molecular lifetime in the nanosecond region (decay of excited state population). However, the single molecule excitation dephasing (decay of ground-state excited state off-diagonal density matrix elements) has been fixed below 1 ps. Such a model of dissipation also implies the absence of exciton relaxation due to emission and absorption of vibrational quanta.

Following the quantum master equation we may write

$$\frac{\partial}{\partial t}\langle \hat{O} \rangle = \text{tr}\left\{ \frac{\partial}{\partial t}\hat{\rho}(t)\hat{O} \right\} = \frac{i}{\hbar}\langle [H(t), \hat{O}]_- \rangle - \langle \tilde{\mathcal{D}}\hat{O} \rangle. \tag{11}$$

The modified dissipative superoperator follows as

$$\tilde{\mathcal{D}}\hat{O} = \sum_m \frac{k_m}{2}([B_m^+ B_m, \hat{O}]_+ - 2B_m^+ \hat{O} B_m). \tag{12}$$

Noting the general type of equations of motion (11) we easily derive equations for different types of $\hat{O}$. Identifying this operator first with B_m^+ we obtain (for details see [18])

$$\frac{\partial}{\partial t}\langle B_m^+\rangle = \frac{i}{\hbar}E_m\langle B_m^+\rangle + \frac{i}{\hbar}\sum_k J_{km}\langle B_k^+(1-2B_m^+B_m)\rangle + \frac{i}{\hbar}R_m^*\langle(1-2B_m^+B_m)\rangle - \frac{k_m}{2}\langle B_m^+\rangle. \tag{13}$$

In a next step we consider the case $\hat{O} = B_m^+ B_m$ and arrive at

$$\frac{\partial}{\partial t}\langle B_m^+B_m\rangle = \frac{i}{\hbar}\sum_k(J_{km}\langle B_k^+B_m\rangle - J_{mk}\langle B_m^+B_k\rangle) + \frac{i}{\hbar}R_m^*\langle B_m\rangle - \frac{i}{\hbar}R_m\langle B_m^+\rangle - k_m\langle B_m^+B_m\rangle. \tag{14}$$

According to the derived equation, next, we have to consider $\hat{O} = B_m^+ B_n$ $(m \neq n)$,

$$\begin{aligned}\frac{\partial}{\partial t}\langle B_m^+B_n\rangle = {}& \frac{i}{\hbar}(E_m - E_n)\langle B_m^+B_n\rangle + \frac{i}{\hbar}\sum_k J_{km}\langle(1-2B_m^+B_m)B_k^+B_n\rangle - \frac{i}{\hbar}\sum_k J_{nk}\langle B_m^+B_k(1-2B_n^+B_n)\rangle \\ & + \frac{i}{\hbar}R_m^*\langle(1-2B_m^+B_m)B_n\rangle - \frac{i}{\hbar}R_n\langle B_m^+(1-2B_n^+B_n)\rangle - \frac{k_m+k_n}{2}\langle B_m^+B_n\rangle. \end{aligned}\tag{15}$$

Obviously, the three types of equations do not form a closed set for $\langle B_m^+\rangle$, $\langle B_m^+B_m\rangle$, and $\langle B_m^+B_n\rangle$. Expectation values with three and four transition operators appear accounting for the correlation of two excitations, for example. We will ignore such higher correlations in the following and focus on the most simple but nontrivial case of nonlinear kinetic equations describing EET. Therefore, a decoupling scheme is used where the operator expression of type $1-2B_m^+B_m$ whenever it appears is replaced by its expectation value $\langle 1-2B_m^+B_m\rangle$ [27]. This expectation value coincides with the so-called population inversion $P_{mg} - P_{me}$ between the ground and the excited state of molecule m. It controls energy transfer among the molecules if more than a single excitation is present in the system (see also below).

While carrying out this decoupling it also would be of interest how to arrive at the standard Förster-theory of EET. In order to get this approximate description it suffices to compute $\langle B_m^+B_n\rangle$ in the lowest order in J_{mn} and insert the result into the equation for $\langle B_m^+B_m\rangle$. If, simultaneously, the expectation values $\langle 1-2B_m^+B_m\rangle$ have been set equal to 1 and the terms $\sim R_m$ are neglected we have obtained a standard rate equation. However, it includes a rather crude version of the EET rates, what is caused by the simple model of dissipation used here (cf. also the discussion in [18]).

To present the equations of motion derived according to the suggested decoupling scheme we introduce a number of abbreviations. The transition amplitude is written as

$$\beta_m = \langle B_m^+\rangle. \tag{16}$$

The molecular excited state population is

$$P_m = \langle B_m^+B_m\rangle, \tag{17}$$

and we introduce

$$W_{mn} = (1-\delta_{m,n})\langle B_m^+B_n\rangle, \tag{18}$$

which is completely off-diagonal with respect to the two molecular indices. Furthermore, we set $\omega_m = E_m/\hbar$, $\tilde{\omega}_m = \omega_m + ik_m/2$, $j_{mn} = J_{mn}/\hbar$, $r_m = R_m/\hbar$, and $\tilde{\omega}_{mn} = \tilde{\omega}_m - \tilde{\omega}_n^*$. It results in the following set of equations of motion:

$$\frac{\partial}{\partial t}\beta_m = i\tilde{\omega}_m\beta_m + i\sum_k j_{km}(1-2P_m)\beta_k + ir_m^*(1-2P_m), \tag{19}$$

$$\frac{\partial}{\partial t}P_m = -\frac{1}{\tau_m}P_m + 2\mathrm{Im}\sum_n j_{mn}W_{mn} + 2\mathrm{Im}r_m\beta_m, \tag{20}$$

and

$$\begin{aligned}\frac{\partial}{\partial t}W_{mn} = {}& i\tilde{\omega}_{mn}W_{mn} - ij_{nm}(P_m - P_n) \\ & + i\sum_{k\neq n} j_{km}(1-2P_m)W_{kn} - i\sum_{k\neq m} j_{nk}(1-2P_n)W_{mk} \\ & + ir_m^*(1-2P_m)\beta_n^* - ir_n(1-2P_n)\beta_m. \end{aligned}\tag{21}$$

To obtain the last equation we noticed $\langle B_k^+B_n\rangle = \delta_{k,n}P_n + (1-\delta_{k,n})W_{kn}$. Now, we have a closed system for β_m, P_m, and W_{mn}. Note also that the term $-k_mP_m$ has been replaced by $1/\tau_m \times P_m$. Therefore, $k_m/2$ is considered as a pure dephasing rate while τ_m represents the molecular excited state lifetime located in the ns region (we introduce a common quantity τ_{mol} identical for all molecules).

To arrive at the final working equations we just carry out the so-called rotating wave approximation (RWA) which removes from the kinetic equation terms oscillating with ω_0 or multiples of it. We set $r_m(t) = -\exp(-i\omega_0 t)\times\Omega_m(t) + \mathrm{c.c.}$ with $\Omega_m(t) = \mathbf{n}\cdot\mathbf{d}_m E(t)/\hbar$, and introduce $\beta_m(t) = \exp(i\omega_0 t)\times b_m(t)$.

Then, the RWA gives

$$\frac{\partial}{\partial t}b_m = i(\tilde{\omega}_m - \omega_0)b_m + i\sum_n j_{nm}(1-2P_m)b_n - i\Omega_m^*(1-2P_m), \tag{22}$$

$$\frac{\partial}{\partial t}P_m(t) = -\frac{1}{\tau_m}P_m(t) + 2\mathrm{Im}\sum_n j_{mn}W_{mn}(t) - 2\Omega_m(t)\mathrm{Im}b_m(t), \tag{23}$$

and

$$\frac{\partial}{\partial t}W_{mn}(t) = i\tilde{\omega}_{mn}W_{mn}(t) - ij_{nm}(P_m(t)-P_n(t)) + i\sum_{k\neq n} j_{km}(1-2P_m(t))W_{kn}(t) - i\sum_{k\neq m} j_{nk}(1-2P_n(t))W_{mk}(t)$$
$$-i\Omega_m^*(t)(1-2P_m(t))b_n^*(t) + i\Omega_n(t)(1-2P_n(t))b_m(t). \tag{24}$$

Since the system is in its ground state before optical excitation the equations are solved in using the following initial conditions:

$$b_m(0) = P_m(0) = W_{mn}(0) = 0. \tag{25}$$

III. PHOTOINDUCED EXCITATION ENERGY DYNAMICS

In the following photoinduced excitation energy kinetics in a regular and linear chain of molecules will be discussed. We do not focus on a particular type of molecule or polymer but choose typical values of the various parameters which are slightly varied (cf. Table I). The molecular excitation energy $E_n = E_{\mathrm{mol}}$ should be identical for all molecules in a chain of up to $N_{\mathrm{mol}} = 25$ molecules. The transition dipole moments d_{mol} are also all identical and take the value of 8 D. Moreover, we assume that the field polarization $\mathbf{n}_E$ is always parallel to the actual dipole orientation.

In order to vary the excitonic coupling and thus the exciton spectrum we change the distance Δ_{mol} among the molecules introducing the values 1.2, 1.5, and 2.5 nm. The nearest neighbor excitonic coupling $J(\Delta_{\mathrm{mol}})$ amounts to the following values. Choosing an H-aggregate configuration we obtain $J(1.2\,\mathrm{nm}) \approx 23$ meV, $J(1.5\,\mathrm{nm}) \approx 12$ meV, and $J(2.5\,\mathrm{nm}) \approx 2.6$ meV. In the case of a J-aggregate the sign changes and the absolute value doubles. Focusing on a linear chain with nearest neighbor coupling only, the exciton energies follow as $\mathcal{E}_\alpha - E_{\mathrm{mol}} = 2J\cos\alpha$ with $\alpha = \pi j/(N_{\mathrm{mol}}+1)$ ($j = 1,\ldots,N_{\mathrm{mol}}$) and the whole exciton spectrum covers the range between $E_{\mathrm{mol}} - 2J$ and $E_{\mathrm{mol}} + 2J$.

TABLE I. Used parameters.

N_{mol}	10–25
E_{mol}	2.6 eV
d_{mol}	8 D
$\hbar k_{\mathrm{mol}}$	3 meV
τ_{mol}	1 ns
Δ_{mol}	1.2, 1.5, 2.5 nm
ω_0	Varied around $E_{\mathrm{mol}}/\hbar$
E_0	10^6–10^8 V/m
τ_{p}	20 fs to 2 ps

A. Preliminary considerations

Before presenting the results of our numerical computations we consider some simple reference cases where an analysis helps to understand the following simulation results. An essential quantity to judge the degree of excitation would be the total excited state population,

$$P_{\mathrm{tot}}(t) = \sum_m P_m(t). \tag{26}$$

Its upper limit is N_{mol} which is reached if all molecules are in their excited state with probability 1. While we have in mind the investigation of multiple excitations, standard exciton theory considers the singly excited state of the molecular system. The most general type of a singly excited state would be $|\phi_1\rangle = \sum_m c(m)B_m^+|\phi_g\rangle$.

The singly excited eigenstate of H_{exc} is the single exciton state $|\alpha\rangle = \sum_m c_\alpha(m)B_m^+|\phi_g\rangle$ with energy $\mathcal{E}_\alpha = \hbar\Omega_\alpha$. The most general type of time-dependent singly excited state can be expanded by the exciton states. It results the formation of an excitonic wave packet,

$$|\phi_1(t)\rangle = U(t)|\phi_1(0)\rangle = \sum_\alpha A_\alpha e^{-i\Omega_\alpha t}|\alpha\rangle. \tag{27}$$

We use this state to compute the time dependence of W_{mn}, Eq. (18), and obtain

$$W_{mn}(t) = \langle\phi_1(t)|B_m^+B_n|\phi_1(t)\rangle = \sum_{\alpha,\beta} c_\alpha^*(m)c_\beta(n)A_\alpha^*A_\beta e^{i\Omega_{\alpha\beta}t}. \tag{28}$$

Accordingly, $W_{mn}(t)$ [and also $P_m(t)$] oscillates with the different excitonic transition frequencies $\Omega_{\alpha\beta} = \Omega_\alpha - \Omega_\beta$. A Fourier analysis of $W_{mn}(t)$ or $P_m(t)$ would indicate this. Therefore, one should consider the equation for W_{mn} in the case of weak excitation ($P_m \ll 1$) where we can remove all terms proportional to P_m. Now we expect that the solution reproduces the above given expression. However, in the general case j_{km} is replaced by $j_{km}(1-2P_m)$ and j_{nk} by $j_{nk}(1-2P_n)$. Effectively, the magnitude of the excitonic coupling is reduced if the excitation density is increased.

Finally, weak optical excitation is considered by a direct solution of the time-dependent Schrödinger equation defined by $H(t)$, Eq. (1). To stay at the weak excitation limit the solution is derived in the first order with respect to the exciting

field included in $H_{\rm field}(t)$, Eq. (5),

$$|\psi(t)\rangle = U(t,t_0)|\psi(t_0)\rangle \approx U_{\rm exc}(t-t_0)\Big\{1-\frac{i}{\hbar}\int_{t_0}^{t} d\tau\; U^{+}_{\rm exc}(\tau-t_0) \times H_{\rm field}(\tau)U_{\rm exc}(\tau-t_0)\Big\}|\phi_g\rangle. \quad (29)$$

The initial state is the molecular system ground state. The time-evolution operator of the exciton system takes the form $U_{\rm exc}(t) = \exp(-iH_{\rm exc}t/\hbar)$. The expression in the curly bracket of the above equation represents the first-order expansion of the external field induced S operator. We expand the time-dependent wave function with respect to exciton states,

$$\langle\alpha|\psi(t)\rangle = A_\alpha(t) = -\frac{i}{\hbar}\int_{t_0}^{t} d\tau\; e^{-i\Omega_\alpha(t-\tau)}\langle\alpha|H_{\rm field}(\tau)|\phi_g\rangle \approx \frac{i}{\hbar}\int_{t_0}^{t} d\tau\; e^{-i\Omega_\alpha(t-\tau)} d_\alpha E(\tau) e^{-i\omega_0\tau}. \quad (30)$$

The τ integral can be easily computed in the limit $t\to\infty$ and $t_0\to-\infty$ [note also $\tau - t_{\rm p}\to\tau$ and Eq. (7) for the field envelope]:

$$A_\alpha(t\to\infty) = \frac{i}{\hbar}\sqrt{\pi\tau_{\rm p}^2/2}\, d_\alpha E_0 e^{-i\Omega_\alpha t + i(\Omega_\alpha-\omega_0)t_{\rm p}} \times e^{-\tau_{\rm p}^2(\Omega_\alpha-\omega_0)^2/8}. \quad (31)$$

Besides the dependence on the exciton transition dipole moments $d_\alpha = \mathbf{d}_\alpha\cdot\mathbf{n}_E$ the magnitude of the expansion coefficients A_α is mainly determined by $\exp[-\tau_{\rm p}^2(\Omega_\alpha-\omega_0)^2/8]$. If ω_0 coincides with a particular exciton level the factor equals 1; $\exp[-\tau_{\rm p}^2(\Omega_\alpha-\omega_0)^2/8]$ immediately becomes smaller than 1 if the pulse duration $\tau_{\rm p}$ is large and if ω_0 deviates a little bit from the actual exciton level. Large means that $\tau_{\rm p}$ is much larger than the inverse of the frequency width of the exciton band ($\tau_{\rm p}\gg 1/\Omega_{\alpha\beta}$). If the pulse is short $\exp[-\tau_{\rm p}^2(\Omega_\alpha-\omega_0)^2/8]$ stays close to 1 although ω_0 may deviate from Ω_α. Different exciton levels are excited simultaneously. An excitonic wave packet is formed. Respective examples are discussed in the subsequent section.

B. Excitation energy dynamics

We consider the temporal behavior of the molecular excited state populations after laser pulse excitation. To have reference data, Fig. 2 displays the behavior of an isolated molecule not coupled to other molecules. The molecule is excited by a 20-fs long pulse and with different values of the field amplitude. As long as the latter is sufficiently low the excited state population P_m follows the laser pulse and stays at its final value (remember that the excited state lifetime amounts to 1 ns). For larger field strength one or two Rabi oscillations appear covering a complete excitation of the molecule ($P_m\approx 1$) and a subsequent induced depopulation (the oscillation of P_m slows down with increasing pulse duration).

The just discussed data for a pulse with $\tau_p = 20$ fs shall be confronted with those of Fig. 3. Here, the P_m of a chain of 10 molecules are drawn for the three different values of the

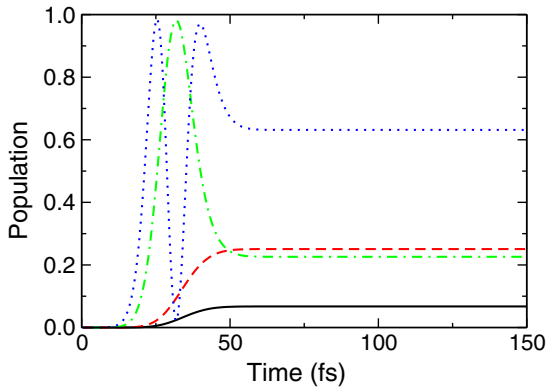

FIG. 2. $\tau_p = 20$ fs laser-pulse-induced excited state population of an isolated molecule (resonant excitation $\hbar\omega_0 = E_{\rm mol}$). Black solid line, $E_0 = 5\times10^7$V/m; red dashed line, $E_0 = 10^8$V/m; green chain dotted line, $E_0 = 5\times10^8$V/m; and blue dotted line, $E_0 = 10^9$V/m.

intermolecular distance, i.e., the excitonic coupling is changed. The chosen field strength corresponds to the black curve in the upper panel of Fig. 2 indicating that no Rabi oscillations will appear. Instead, the oscillations of the excited state populations visible in all panels of Fig. 3 are the result of EET (the oscillation period gets larger with increasing intermolecular distance, i.e., decreasing coupling). Because of the regular structure of the chain we observe symmetric populations $P_m = P_{N_{\rm mol}+1-m}$. During laser-pulse excitation all molecules get excited ($P_m\approx 0.06$). Afterward EET from the terminal sites of the chain to the center set in leading to the peak value of $P_5 = P_6$. We quote the so-called coherent transfer time $t_{\rm coh} = \pi\hbar/J$ (J denotes the nearest neighbor excitonic coupling with respective values presented beforehand). Related to the actual value of $\Delta_{\rm mol}$ we get $t_{\rm coh}(1.2\,{\rm nm})\approx 88$ fs, $t_{\rm coh}(1.5\,{\rm nm})\approx 176$ fs, and $t_{\rm coh}(2.5\,{\rm nm})\approx 807$ fs. Such oscillation periods can be identified in the three panels of Fig. 3. Finally, dephasing results in an equal distribution of excitation of all molecules. These steady-state values $P_m^{\rm (ss)}$ of the excited state populations increase slightly with increasing $\Delta_{\rm mol}$.

This can be understood as follows. The resulting decrease of J decreases the width of the exciton band. Since we chose $\hbar\omega_0 = E_{\rm mol}$ we excite at the center of the exciton band with a full width at half maximum of ≈80 meV (corresponding to the 20-fs pulse duration). Accordingly, the excited state population increases if the exciton band is shrunk.

Figures 4 and 5 demonstrate the effect of the pulse duration. To stay comparable we took the same value of the pulse area $\bar{E} = \int dt\; E(t) = E_0\sqrt{\pi/4\ln 2}\times\tau_{\rm p}$. Figure 4 displays the effect of a 100-fs long excitation and Fig. 5 shows data for $\tau_{\rm p} = 1$ ps. Both figures correspond to $\Delta_{\rm mol} = 1.2$ nm. As long as the pulse duration is comparable to the coherent transfer time $t_{\rm coh}$ (88 fs here), EET among the different molecules results in oscillations of the excited state populations (Fig. 4). For larger pulse durations the P_m continuously move to their steady-state values $P_m^{\rm (ss)}$ (Fig. 5). For a given value of $\Delta_{\rm mol}$ the $P_m^{\rm (ss)}$ decrease with increasing pulse duration. Again, the decreasing spectral width of the pulse with increasing $\tau_{\rm p}$ localizes excitation more and more at the center of the exciton band. Since oscillator strength is localized at the upper level in the considered H aggregate, we notice decreasing values of the

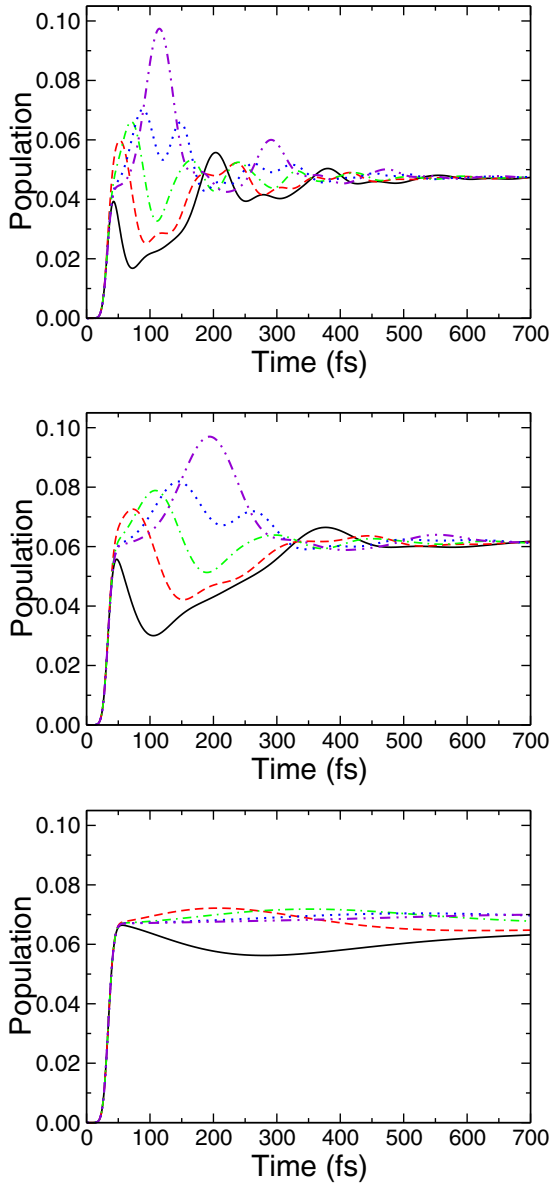

FIG. 3. Laser-pulse-induced energy transfer dynamics in a chain of 10 molecules (H-aggregate configuration, $\tau_p = 20$ fs, $E_0 = 5 \times 10^7$ V/m, $\hbar\omega_0 = E_{\rm mol}$). Upper panel, $\Delta_{\rm mol} = 1.2$ nm; middle panel, $\Delta_{\rm mol} = 1.5$ nm; lower panel, $\Delta_{\rm mol} = 2.5$ nm. Black solid line, $P_1 = P_{10}$; red dashed line, $P_2 = P_9$; green chain dotted line, $P_3 = P_8$; blue dotted line, $P_4 = P_7$; violet chain double dotted line, $P_5 = P_6$.

$P_m^{(\rm ss)}$. However, if we compare molecular chains with different $\Delta_{\rm mol}$ the increase of the intermolecular distance decreases J. The resulting shrinkage of the exciton band increases the excitation for a fixed pulse duration.

Next, we turn to the case of higher field strengths to see how Rabi oscillations interfere with population oscillations due to EET. Figure 6 displays the case of $\tau_p = 20$ fs and, again, a chain of 10 molecules with $\Delta_{\rm mol} = 1.2$ nm is considered. Therefore, these results have to be confronted with those shown in the upper panel of Fig. 3. Choosing $E_0 = 10^8$ V/m only the overall population is increased compared to Fig. 3. However, a value of $E_0 = 5 \times 10^8$ V/m induces a Rabi oscillation which is followed by less pronounced population oscillations. The

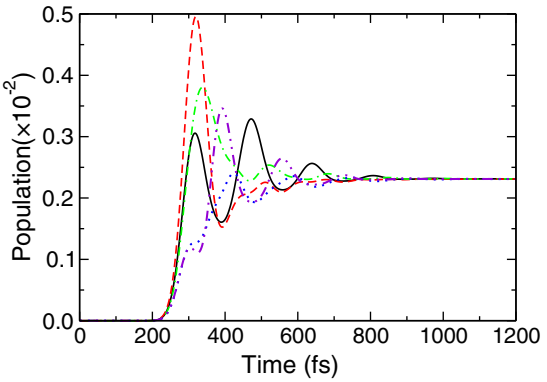

FIG. 4. $\tau_p = 100$ fs laser-pulse-induced energy transfer dynamics in a chain of 10 molecules (H-aggregate configuration, $\Delta_{\rm mol} = 1.2$ nm, $E_0 = 10^7$ V/m). Black solid line, $P_1 = P_{10}$; red dashed line, $P_2 = P_9$; green chain dotted line, $P_3 = P_8$; blue dotted line, $P_4 = P_7$; violet chain double dotted line, $P_5 = P_6$.

strong and simultaneous increase of all P_m near a value of 1 somewhat suppresses these oscillations. The effect of an increasing pulse duration is shown in the subsequent Fig. 7. Again, if $\tau_p > t_{\rm coh}$ (lower panel) any population oscillation disappears.

IV. OPTICAL RESPONSE

The basic equations for $b_m(t)$, $P_m(t)$, and $W_{mn}(t)$ contain the terms $\sim 2P_n$ as nonlinearities. These terms decrease the energy transfer coupling J_{mn} and we can expect a change of the exciton spectrum. In the framework of the present description the spectral changes cannot be calculated directly by solving an eigenvalue equation. We suggest an alternative way to find signatures of these spectral changes, finally in the detection of the emission spectrum or the transient absorption of a pump-probe experiment.

This alternative way uses changes of the absorption of an exciting laser pulse (pump beam) if the exciton spectrum changes. Since we concentrate on a sub-ps excitation the

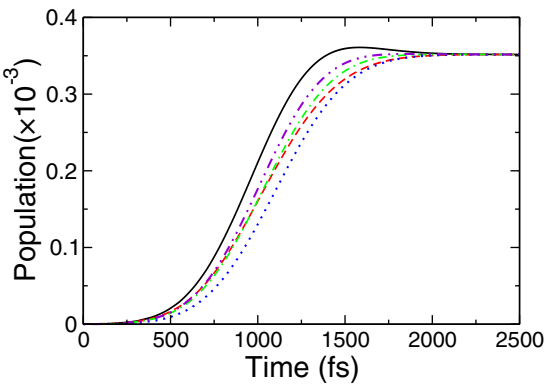

FIG. 5. $\tau_p = 1$ ps laser-pulse-induced energy transfer dynamics in a chain of 10 molecules (H-aggregate configuration, $\Delta_{\rm mol} = 1.2$ nm, $E_0 = 10^6$ V/m). Black solid line, $P_1 = P_{10}$; red dashed line, $P_2 = P_9$; green chain dotted line, $P_3 = P_8$; blue dotted line, $P_4 = P_7$; violet chain double dotted line, $P_5 = P_6$.

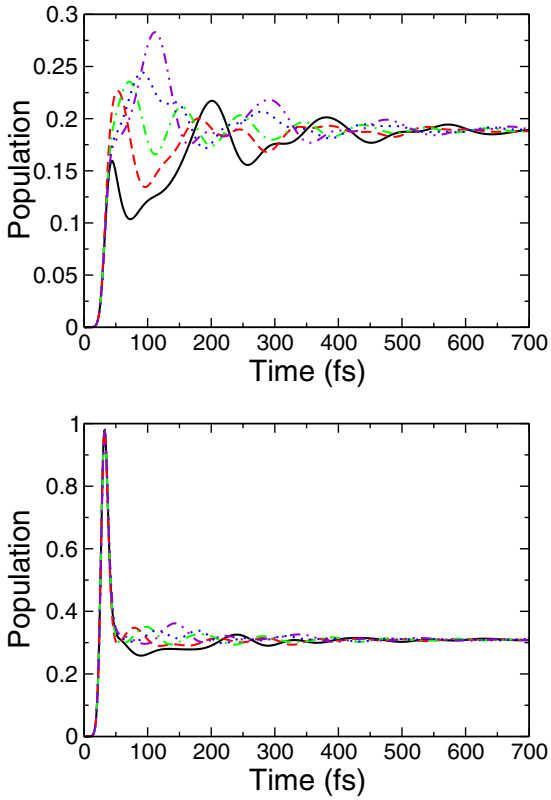

FIG. 6. Laser-pulse-induced energy transfer dynamics in a chain of 10 molecules (H-aggregate configuration, $\Delta_{\rm mol} = 1.2$ nm, $\tau_p = 20$ fs). Upper panel, $E_0 = 10^8$ V/m; lower panel, $E_0 = 5 \times 10^8$ V/m.

spectral changes shall be detected via an intermediate steady state of the molecular excited state populations $P_m^{(\rm ss)}$ which are formed in a time region of 1–100 ps. If we draw the $P_m^{(\rm ss)}$ which are identical for all molecules versus the exciting photon energy $\hbar\omega_0$ large values are expected if $\hbar\omega_0$ matches an exciton energy $\mathcal{E}_\alpha$. If this is repeated for different pulse intensities the changing exciton spectrum should become visible.

We first calculate the steady-state populations versus $\hbar\omega_0$ and for different field-strengths E_0 to later on explain the relation to emission and transient absorption spectra. To make the total degree of excitation also visible we do not discuss the individual populations $P_m^{(\rm ss)}$ but the total excited state population,

$$P_{\rm tot}^{(\rm ss)} = \sum_m P_m^{(\rm ss)}, \tag{32}$$

of the molecular complex.

Figure 8 shows respective results. We present curves for a chain of 10 molecules either in a H- or J-aggregate configuration (computations for 25 molecules gave similar results). $P_{\rm tot}^{(\rm ss)}$ drawn versus photon energy of the exciting laser pulse displays different peaks which change their spectral position when increasing the laser pulse intensity. As it has to be expected the peaks are located above $E_{\rm mol} = 2.6$ eV for the H-aggregate configurations and below $E_{\rm mol}$ for the J-aggregate configurations (there are more peaks for the longer chain).

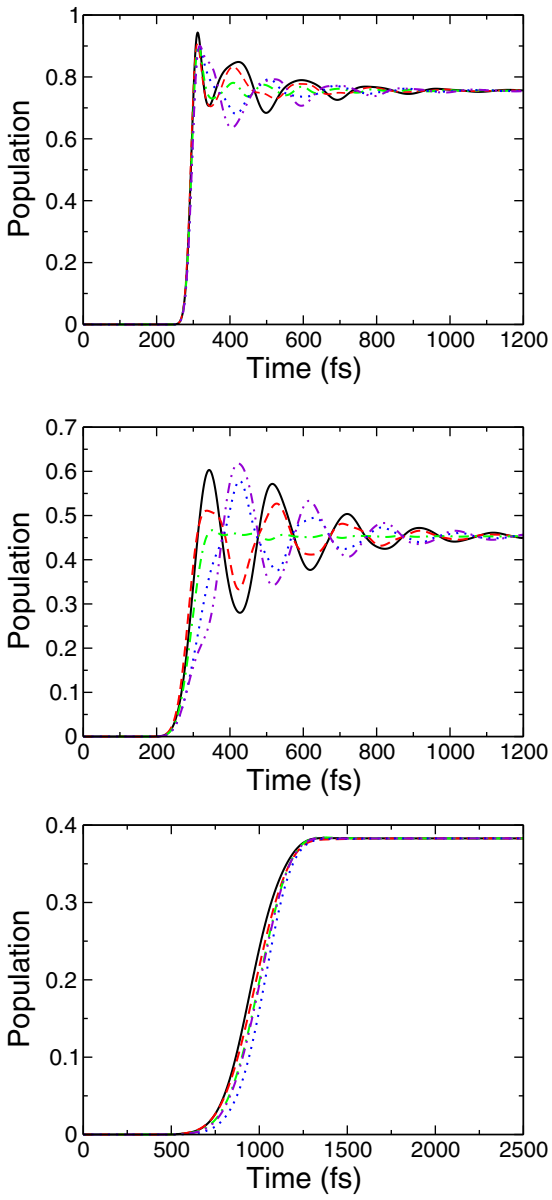

FIG. 7. Laser-pulse-induced energy transfer dynamics in a chain of 10 molecules (H-aggregate configuration, $\Delta_{\rm mol} = 1.2$ nm). Upper panel, $\tau_p = 50$ fs, $E_0 = 2 \times 10^8$ V/m; middle panel, $\tau_p = 100$ fs, $E_0 = 10^8$ V/m; lower panel, $\tau_p = 500$ fs, $E_0 = 2 \times 10^7$ V/m,

Increasing the laser-pulse field strength the peaks of the H-aggregate configuration (upper panel in Fig. 8) move to lower energies. The behavior is opposite for the chain with J-aggregate configuration. Here, peaks above $E_{\rm mol}$ are also visible which move downwards in energy. This indicates a compression of the whole exciton band which has to be expected if the energy transfer couplings J_{mn} are effectively reduced.

As described in detail in the Appendix the transient absorption signal as well as the emission intensity become proportional to the $P_m^{(\rm ss)}$ and in the present case (of a system of identical molecules) proportional to $P_{\rm tot}^{(\rm ss)}$. So drawing the probe pulse signal $S_{\rm pr}$ or the photon emission intensity $I_{\rm emi}$ versus the photon energy $\hbar\omega_0$ of the exciting laser pulse and

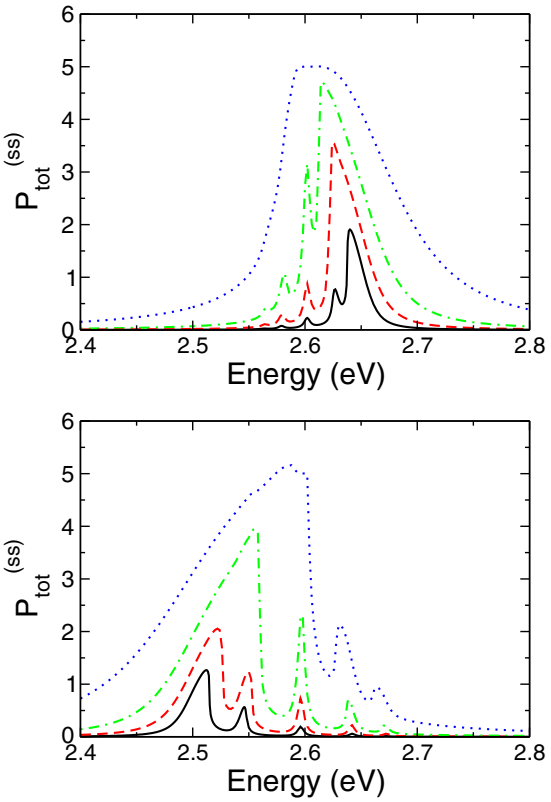

FIG. 8. Steady-state value $P_{\rm tot}^{\rm (ss)}$ of the total excitation of a 10 molecule chain versus photon energy $\hbar\omega_0$ of the exciting laser pulse (pulse duration $\tau_p = 2$ ps, molecular distance $\Delta_{\rm mol} = 1.2$ nm). Upper panel, H-aggregate configuration; lower panel, J-aggregate configuration. Variation of the laser pulse field strength. Black solid line, $E_0 = 5 \times 10^6$ V/m; red dashed line, $E_0 = 10^7$ V/m; green chain-dotted line, $E_0 = 2 \times 10^7$ V/m; blue dotted line, $E_0 = 5 \times 10^7$ V/m.

for different field strengths, it should result in similar curves as drawn in Fig. 8.

One would also expect that the emission line shape $I_{\rm emi}$ if drawn versus the energy $\hbar\omega$ of the emitted photons, directly displays the changed exciton spectrum. However, as detailed in the Appendix, this is not the case. The completely relaxed exciton state and the random character of photon emission avoids this. In contrast, we have to note the coherent character of optical excitation also included in the equation of motion for $W_{mn} = \langle B_m^+ B_n \rangle$. This guarantees that the excitation process notices the intensity-dependent change of the exciton spectrum as displayed in Fig. 8.

V. CONCLUSIONS

The nonlinear response of a regular 1D molecular system on ultrafast and strong optical excitation has been discussed. To avoid exciton-exciton annihilation as a dominant quenching process we considered a system where the ground-state–first-excited-state transition energy is smaller than the first-excited-state–second-excited-state transition energy. Now, resonant optical excitation may result in the creation of many excitons. To investigate such dense Frenkel-exciton systems we applied a reference approximation leading to a mean-field description and neglected vibrational contributions. An interference of Rabi-type oscillations with oscillations caused by excitation energy transfer dominates the temporal behavior after laser pulse excitation. If the total degree of excitation is analyzed versus the energy of exciting photons a shrinkage of the exciton spectrum with increasing excitation intensity appears. We demonstrated a possible detection of this effect in the framework of a two-color pump-probe experiment and the measurement of photon emission. Of course, the importance of the described behavior can be only judged if an assessment of the used mean-field description has been carried out. Improved decouplings of the hierarchical system of equations of motion are under investigation.

ACKNOWLEDGMENTS

This work has been supported by the National Natural Science Foundation of China (Grant No. 11174029) (L.W.) and the Deutsche Forschungsgemeinschaft through Sfb 951 (V.M.).

APPENDIX A: TRANSIENT ABSORPTION SPECTRUM

We consider the probe-pulse transient absorption within a two-color pump-probe experiment and focus on the sequential regime without any temporal overlap of the pump and the probe pulse. This corresponds to the detection of the steady-state situation of the excitonic system after optical excitation with the laser pulse introduced in Eqs. (5) and (6). The excitation (pumping) appears at carrier frequency ω_0 and with field envelope $E(t)$. To distinguish both quantities from those belonging to the probe pulse we denote the probe pulse frequency as $\omega_{\rm pr}$ and the respective envelope as $E_{\rm pr}(t)$. While the photon energy of the pump pulse is close to E_m that of the probe pulse shall be in resonance to $\mathcal{E}_m = E_{mf} - E_{me} \neq E_m$. So, the population of the first excited state of the molecules can be probed via excited state absorption.

Following the standard scheme of determining transient absorption spectra (see [16] and references therein) we calculate the probe-pulse transient absorption signal according to (note the application of the slowly varying amplitude approximation)

$$S_{\rm pr}(t) = 2V\omega_{\rm pr}{\rm Im}[E_{\rm pr}^*(t)P_{\rm pr}(t)]. \tag{A1}$$

If integrated with respect to time it gives the energy gain the molecular system experiences due to the complete probe-field action (V denotes the sample volume). Since the probe pulse shall act after an (intermediate) steady state has been established due to the pump pulse action, the probe-pulse-induced polarization $P_{\rm pr}(t)$ is computed in a linear response approach [28],

$$P_{\rm pr}(t) = \int d\bar{t}\; e^{i\omega_{\rm pr}(t-\bar{t})} R_{\rm pr}(t,\bar{t}) E_{\rm pr}(\bar{t}). \tag{A2}$$

The response function is defined with respect to the pump-pulse-induced excited state. It is accounted for by the steady-state form $\hat{\rho}^{\rm (ss)}$ of the density operator. Moreover, the response function depends on the time difference only and takes the

form,

$$R_{\rm pr}(t) = \frac{i}{\hbar}\theta(t){\rm tr}\{\hat{\mu}\mathcal{U}(t)[\hat{\mu},\hat{\rho}^{(\rm ss)}]_-\}. \quad \text{(A3)}$$

The dipole operator $\hat{\mu}$ now covers contributions due to the higher excited state φ_{mf} according to

$$\hat{\mu}_f = \sum_m \mathbf{p}_m D_m^+ + {\rm H.c.}. \quad \text{(A4)}$$

We restricted ourselves to the transition between φ_{me} and φ_{mf} with the related transition dipole moment $\mathbf{p}_m$ and transition operator $D_m^+ = |\varphi_{mf}\rangle\langle\varphi_{me}|$. Since pump and probe frequency are out of resonance the response function $R_{\rm pr}$ can be computed in restricting $\hat{\mu}$ to $\hat{\mu}_f$. The time dependence of $R_{\rm pr}$ is caused by the time-evolution superoperator $\mathcal{U}(t)$ which is the solution of a quantum master equation. In contrast to the quantum master equation (9) used beforehand, here, we can ignore any external field contribution, but have to include in the unitary part the additional Hamiltonian,

$$H_f = \sum_m \mathcal{E}_m D_m^+ D_m. \quad \text{(A5)}$$

The dissipative superoperator, Eq. (10), is extended by

$$\mathcal{D}_f\hat{\rho}(t) = \sum_m \frac{r_m}{2}([D_m^+D_m,\hat{\rho}(t)]_+ - 2D_m\hat{\rho}(t)D_m^+). \quad \text{(A6)}$$

It includes finite lifetimes $1/r_m$ of the higher excited state. In a next step we define

$$\hat{\sigma}(t) = \mathcal{U}(t)[\hat{\mu},\hat{\rho}^{(\rm ss)}]_-, \quad \text{(A7)}$$

and denote the probe-pulse response function as

$$R_{\rm pr}(t) = \frac{i}{\hbar}\theta(t)\sum_m(\mathbf{p}_m{\rm tr}\{D_m^+\hat{\sigma}(t)\} + \mathbf{p}_m^*{\rm tr}\{D_m\hat{\sigma}(t)\}). \quad \text{(A8)}$$

Some algebra gives the initial value according to

$${\rm tr}\{D_m^+\hat{\sigma}(0)\} = \mathbf{p}_m^*{\rm tr}\{\hat{\rho}^{(\rm ss)}(D_m^+D_m - D_mD_m^+)\} = -\mathbf{p}_m^*P_m^{(\rm ss)}. \quad \text{(A9)}$$

We took into consideration that $D_m^+D_m - D_mD_m^+ = |\varphi_{mf}\rangle\langle\varphi_{mf}| - |\varphi_{me}\rangle\langle\varphi_{me}|$ and that $\hat{\rho}^{(\rm ss)}$ only contributes to the steady-state population $P_m^{(\rm ss)}$ of the first excited state.

Since any coupling among the higher excited states and among the higher excited and first excited states are absent it simply follows

$${\rm tr}\{D_m^+\hat{\sigma}(t)\} = -e^{i\tilde{\Omega}_m t}\mathbf{p}_m^*P_{me}^{(\rm ss)}. \quad \text{(A10)}$$

We used $\tilde{\Omega}_m = \mathcal{E}_m/\hbar + ir_m/2$. Note also that ${\rm tr}\{D_m\hat{\sigma}(0)\}$ follows as the negative and conjugated complex version of the expression given beforehand. According to the assumption of a regular chain of molecules any site dependence vanishes and we arrive at

$$R_{\rm pr}(t) = -\frac{i}{\hbar}\theta(t)|\mathbf{p}|^2(e^{i\tilde{\Omega}t} - {\rm c.c.})P_{\rm tot}^{(\rm ss)}, \quad \text{(A11)}$$

with the total excitation $P_{\rm tot}^{(\rm ss)}$, Eq. (32). Obviously, the total probe pulse signal $S_{\rm pr}$ is proportional to $P_{\rm tot}^{(\rm ss)}$.

APPENDIX B: THE EMISSION SPECTRUM

Photoemission from excited molecular states has been discussed by us beforehand at several places (note our earlier work in [26,29]). The emission spectrum is defined as the number of photons with frequency ω emitted per time,

$$F(\omega;t) = \frac{V\omega^2}{(2\pi c)^3}\sum_\lambda\int do\ R_\lambda(\omega;t). \quad \text{(B1)}$$

The expression incorporates the rate $R_\lambda(\omega;t) = R_{\lambda\mathbf{k}}(t)$ determining the number of photons emitted per time into the state with polarization λ and wave vector $\mathbf{k}$ ($\omega = c|\mathbf{k}|$; V is the quantization volume and the solid angle integration has been abbreviated by $\int do$). For further use we introduce the line-shape function $I_{\rm emi}$ according to $F(\omega;t) = 4\omega^3/3\pi c^3\hbar \times I_{\rm emi}(\omega;t)$. A second-order computation of $I_{\rm emi}$ with respect to the molecule-photon coupling, a concentration on resonant contributions, and a separation of the two time-dependency results in [26,29],

$$I_{\rm emi}(\omega;t) = {\rm Re}\sum_{m,n} d_m d_n^*\int_0^\infty d\tau\ e^{-i\omega\tau}{\rm tr}\{B_m^+(\mathcal{U}(\tau)B_n\hat{\rho}(t))\}. \quad \text{(B2)}$$

Here, $\mathcal{U}(\tau)$ is the time-evolution superoperator which generates the initially introduced density operator equation (9), but is independent of the exciting laser pulse. Thus, we do not consider any interference effect between optical excitation accounted for when computing the density operator $\hat{\rho}(t)$ and photon emission spectrum generated by $\mathcal{U}(\tau)$.

Next, we focus on the steady-state version $\hat{\rho}^{(\rm ss)}$ of the density operator, which is reached at a time after the laser pulse action is over and after the system has been relaxed. To compute the respective emission spectrum we introduce

$$\bar{\beta}_m(\tau;n) = {\rm tr}\{B_m^+\hat{\sigma}_n(\tau)\} = \langle B_m^+\rangle_{\sigma(n)}, \quad \text{(B3)}$$

with

$$\hat{\sigma}_n(\tau) = \mathcal{U}(\tau)B_n\hat{\rho}^{(\rm ss)}. \quad \text{(B4)}$$

The index $\sigma(n)$ at the bracket indicates the averaging with $\hat{\sigma}_n$ instead of $\hat{\rho}$. The initial value of $\bar{\beta}_m$ can be written as

$$\bar{\beta}_m(0;n) = \langle B_m^+B_n\rangle = {\rm tr}\{\hat{\rho}^{(\rm ss)}B_m^+B_n\} = \delta_{m,n}P_m^{(\rm ss)} + (1-\delta_{m,n})W_{mn}^{(\rm ss)} = P_{\rm tot}^{(\rm ss)}/N_{\rm mol}. \quad \text{(B5)}$$

The off-diagonal quantities $W_{mn}^{(\rm ss)}$ vanish and the whole expression becomes proportional to the total degree of excitation $P_{\rm tot}^{(\rm ss)}$, Eq. (32). This indicates immediately $I_{\rm emi} \sim P_{\rm tot}^{(\rm ss)}$.

Next, we note that $\bar{\beta}_m$ is identical to β_m except the density operator used for averaging and the initial values. Considering the equation of motion for $\bar{\beta}_m$,

$$\frac{\partial}{\partial\tau}\bar{\beta}_m(\tau;n) = -\frac{i}{\hbar}\langle[H_{\rm exc},B_m^+]_-\rangle_{\sigma(n)} - \langle\tilde{\mathcal{D}}B_m^+\rangle_{\sigma(n)}, \quad \text{(B6)}$$

one can establish the same system of subsequent equations as in the case where one starts with β_m. Since we consider a time region where optical excitation is over (and where a steady state in the molecular system has been established) the

Hamiltonian is reduced to the time-independent part $H_{\rm exc}$. We further introduce the functions,

$$\bar{P}_m = \langle B_m^+ B_m \rangle_{\sigma(n)}, \tag{B7}$$

and

$$\bar{W}_{mn} = (1-\delta_{m,n})\langle B_m^+ B_n \rangle_{\sigma(n)}, \tag{B8}$$

which together with $\bar{\beta}_m$ obey the same equations of motion as β_m, P_m, and W_{mn} except that optical excitation is absent ($r_m = 0$). Therefore, we arrive at

$$\frac{\partial}{\partial\tau}\bar{\beta}_m = i\tilde{\omega}_m\bar{\beta}_m + i\sum_k j_{km}(1-2\bar{P}_m)\bar{\beta}_k, \tag{B9}$$

$$\frac{\partial}{\partial\tau}\bar{P}_m = -k_m\bar{P}_m + 2{\rm Im}\sum_n j_{mn}\bar{W}_{mn}, \tag{B10}$$

and

$$\begin{aligned}\frac{\partial}{\partial\tau}\bar{W}_{mn} = {}& i\tilde{\omega}_{mn}\bar{W}_{mn} - ij_{nm}(\bar{P}_m - \bar{P}_n) \\ & + i\sum_{k\neq n} j_{km}(1-2\bar{P}_m)\bar{W}_{kn} \\ & - i\sum_{k\neq m} j_{nk}(1-2\bar{P}_n)\bar{W}_{mk}.\end{aligned} \tag{B11}$$

To avoid the presence of fast oscillations we change to $\bar{b}_m(\tau;n) = \exp(-i\omega_0\tau)\times\bar{\beta}_m(\tau;n)$. The related equations of motion take the form,

$$\frac{\partial}{\partial t}\bar{b}_m = i(\tilde{\omega}_m - \omega_0)\bar{b}_m + i\sum_n j_{nm}(1-2\bar{P}_m)\bar{b}_n, \tag{B12}$$

and the (time-independent) emission lineshape follows as

$$I_{\rm emi}(\omega) = |d_{\rm mol}|^2 {\rm Re}\int_0^\infty d\tau\; e^{-i(\omega-\omega_0)\tau}\sum_{m,n}\bar{b}_m(\tau;n). \tag{B13}$$

Note the consideration of identical molecules which results in the replacement of $[\mathbf{d}_m\mathbf{d}_n^*]$ by $|d_{\rm mol}|^2$. Finally we quote all types of initial values,

$$\begin{aligned}\bar{P}_m(0;n) &= {\rm tr}\{\hat{\rho}^{(\rm ss)}B_m^+B_mB_n\} = (1-\delta_{m,n}){\rm tr}\{\hat{\rho}^{(\rm ss)}B_m^+B_mB_n\} \\ &\approx (1-\delta_{m,n})P_m^{(\rm ss)}\beta_n^{(\rm ss)*},\end{aligned} \tag{B14}$$

and

$$\begin{aligned}\bar{W}_{mm'}(0;n) &= (1-\delta_{m,m'}){\rm tr}\{\hat{\rho}^{(\rm ss)}B_m^+B_{m'}B_n\} \\ &\approx (1-\delta_{m,m'})(1-\delta_{m',n})W_{mm'}^{(\rm ss)}\beta_n^{(\rm ss)*}.\end{aligned} \tag{B15}$$

They are all proportional to $\beta_n^{(\rm ss)*}$. Since this quantity equals zero, $\bar{P}_m$ and $\bar{W}_{mm'}$ also equal zero at finite time. As a consequence, the emission lineshape becomes independent on the excitation strength because Eq. (B9) always has to be solved with $\bar{P}_m = 0$

Such a result indicates that the completely relaxed steady state is unable to display the excitation-dependent shrinkage of the exciton spectrum. When considering photon emission it is determined by $\bar{\beta}_m$ with the initial value proportional to $P_m^{(\rm ss)}$. In contrast, the formation of $P_{\rm tot}^{(\rm ss)}$ includes coherent excitation of the pump pulse which guarantees spectrum shrinkage.

[1] B. M. Savoie, N. E. Jackson, L. X. Chen, T. J. Marks, and M. A. Ratner, Acc. Chem. Res. **47**, 3385 (2014).
[2] F. C. Spano and C. Silva, Annu. Rev. Phys. Chem. **65**, 477 (2014).
[3] Y. Tamai, H. Ohkita, H. Benten, and S. Ito, J. Phys. Chem. Lett. **6**, 3417 (2015).
[4] S. Reineke, M. Thormschke, B. Lüssem, and K. Leo, Rev. Mod. Phys. **85**, 1245 (2013).
[5] S. Cook, H. Liyuan, A. Furube, and R. Katoh, J. Phys. Chem. C **114**, 10962 (2010).
[6] D. Peckus, A. Devizis, D. Hertel, K. Meerholz, and V. Gulbinas, Chem. Phys. **404**, 42 (2012).
[7] S. Gélinas, J. Kirkpatrick, I. A. Howard, K. Johnson, M. W. B. Wilson, G. Pace, R. H. Friend, and C. Silva, J. Phys. Chem. B **117**, 4649 (2013).
[8] D. C. Dai and A. P. Monkman, Phys. Rev. B **87**, 045308 (2013).
[9] S. F. Völker, A. Schmiedel, M. Holzapfel, K. Renziehausen, V. Engel, and C. Lambert, J. Phys. Chem. C **118**, 17467 (2014).
[10] F. Fennel and S. Lochbrunner, Phys. Rev. B **92**, 140301 (2015).
[11] Y. Yin, T. Qiu, J. Li, and P. K. Chu, Nano Energy **1**, 25 (2012).
[12] P. Berini and I. D. Leon, Nat. Photonics **6**, 16 (2012).
[13] F. C. Spano, Phys. Rev. B **46**, 13017 (1992).
[14] G. Juzeliunas and J. Knoester, J. Chem. Phys. **112**, 2325 (2000).
[15] S. Mukamel and O. Berman, J. Chem. Phys. **119**, 12194 (2003).
[16] S. Mukamel and D. Abramavicius, Chem. Rev. **104**, 2073 (2004).
[17] Y. Zhang and V. May, Phys. Rev. B **89**, 245441 (2014).
[18] V. May, J. Chem. Phys. **140**, 054103 (2014).
[19] D. Han, J. Du, T. Kobayashi, T. Miyatake, H. Tamiaki, Y. Li, and Y. Leng, J. Phys. Chem. B **119**, 12265 (2015).
[20] E. Engel, K. Leo, and M. Hoffmann, Chem. Phys. **325**, 170 (2006).
[21] H. Lin, R. Camacho, Y. Tian, T. E. Kaiser, F. Würthner, and I. G. Scheblykin, Nano Lett. **10**, 620 (2010).
[22] D. Chaudhuri, D. Li, Y. Che, W. Shafran, J. M. Gerton, L. Zang, and J. M. Lupton, Nano Lett. **11**, 488 (2011).
[23] A. Thiessen, D. Würsch, S.-S. Jester, A. Vikas Aggarwal, A. Idelson, S. Bange, J. Vogelsang, S. Höger, and J. M. Lupton, J. Phys. Chem. B **119**, 9949 (2015).
[24] Y. Zhang and V. May, J. Chem. Phys. **142**, 224702 (2015).
[25] M. Richter, M. Gegg, T. S. Theuerholz, and A. Knorr, Phys. Rev. B **91**, 035306 (2015).
[26] Y. Zhang, Y. Zelinskyy, and V. May, J. Nanophot. **6**, 063533 (2012).
[27] We note that the decoupling of $\langle B_m^+B_m\rangle$ according to $\langle B_m^+\rangle\langle B_m\rangle$ which also seems to be possible is incorrect. It replaces $\langle|\varphi_{me}\rangle\langle\varphi_{me}|\rangle$ with $\langle|\varphi_{me}\rangle\langle\varphi_{mg}|\rangle\langle|\varphi_{mg}\rangle\langle\varphi_{mg}|\rangle$ which represents an incorrect upgrading of the original expression.
[28] D. V. Tsivlin, H.-D. Meyer, and V. May, J. Chem. Phys. **124**, 134907 (2006).
[29] L. Wang and V. May, J. Electroanal. Chem. **660**, 320 (2011).